A mathematical framework for the optimal coupling of interdependent critical infrastructures

Andrea Bellè, Adam F. Abdin, Zhiguo Zeng, Yi-Ping Fang, Anne Barros

A mathematical framework for the optimal coupling of interdependent critical infrastructures

Andrea Bellè, Adam F. Abdin, Zhiguo Zeng, Yi-Ping Fang, and Anne Barros

***Abstract*—Critical infrastructures, such as energy systems, transportation and telecommunications networks, are essential for the safety and socio-economic stability of a society. Critical infrastructures are often tightly coupled and interdependent on each other, and the topology of the interdependencies between different systems, also referred to as the coupling interface, plays a key role in terms of their performance and resilience against failures. In case of failures due natural events or deliberate attacks, the design of the coupling interface can strongly impact the systems performance. However, in the existing literature, the issue of the coupling interface design is often addressed approximately. In this work, we propose an optimization-based mathematical approach for designing coupling interfaces between interdependent critical infrastructures under external attacks. Given a set of possible attack scenarios, the proposed approach allows designing a coupling interface such that the interdependent infrastructures are robust against the worst-case realization of performance losses. Using as a case-study interdependent power and gas networks, we show that the proposed method outperforms existing solutions based on network metrics.**

***Index Terms*—defender-attacker-defender, interdependent critical infrastructures, coupling interface, external attacks, power network, gas network**

I. Introduction

A. Motivation

CRITICAL INFRASTRUCTURES (CIs), such as energy systems, transportation and telecommunications networks, are large and complex man-made systems which support vital societal functions and represent a driving force in the socioeconomic development [1]. In fact, many essential services and commodities, such as electricity, public transportation, water and gas supply or telecommunications, are provided by CIs [2]. At the same time, attacks and disruptive events within CIs, such as intentional sabotages, extreme natural hazards or random failures, can cause disruption and considerable negative consequences within a society. For example, the blackout which affected Italy on 28 September 2003 caused over 10 hours of power outages for more than 50 millions people [3].

CIs are not stand-alone isolated systems, but interconnected systems which are interdependent on each other, in terms of functionality, reliability and performance [4]. While these interdependencies increase the operational performance and efficiency of CIs, they often lead to an increased vulnerability [5]. Interdependent networks and systems are intrinsically more fragile than isolated systems [5], as a failure within one infrastructure can spread within other infrastructures and cause multi-sectoral disruption [5], [6], [7]. In addition, it is also known (from network science, see for example [8] or [9]) that the topology of the interdependencies (or, in other words, how interdependent systems are coupled together) can heavily affect the behaviour of interdependent CIs under attacks and disruptive events. In a practical scenario, the way specific components of an infrastructure depend on specific components of another one is a key factor that affects the resilience of the interdependent systems.

It is thus clear that the way we design the topology of the interdependencies, in this work referred to as the coupling interface [10], [11], is a key feature for the resilience of CIs. However, in the existing literature, this issue is addressed seldomly. In fact, the coupling interface is usually considered as a given parameter, and the impact of different interdependency topologies on the systems resilience is not analyzed. Only a few works consider different coupling interfaces in their analysis, relying on topologies based on network metrics. The aim of this article is to bridge this gap by proposing a mathematical programming approach, based on the defender-attacker-defender (DAD) optimization framework [12].

B. Related work

In most of the existing literature, it is common practice to treat the coupling interface between interdependent infrastructures as a known parameter. Many scholars have adopted this strategy, adapting it for different kind of analysis and interdependent infrastructures scenarios. For example, in [13] and [14], the authors optimize defense strategies and post-disaster restoration in interdependent power-gas networks and power-water networks, respectively; in [15] and [16], the authors assess the vulnerability and the resilience, respectively, of interdependent power-gas network under attacks; in [17] and [18], the authors evaluate the vulnerability of railway networks and their interdependent subsystems under disruption scenarios; in [19], disruption and recovery of interdependent power, water and telecommunications networks are modeled. In all of the above works, the coupling interface is a given parameter. In fact, only a limited number of existing works discuss the optimal design of the coupling interface. In [11], the authors propose a heuristic optimization model for designing optimal coupling interfaces between complex urban infrastructure systems against external attacks. The coupling interface is based on traditional network metrics, such as node degree, betweenness, clustering coefficient and Euclidean distance. Interface design between power, gas and water networks is given as an illustrative case-study. A similar approach is presented in [10], where the authors propose a network metrics-based heuristic method to optimize coupling

interfaces against cascading failures and different external attacks scenarios. However, frameworks based on heuristics can not ensure the convergence to a global optimal solution and the final results are highly dependent on the heuristics used .

Other scholars considered the impact of different network metrics-based coupling interfaces on the analysis of interdependent critical infrastructures, mainly for interdependent power and telecommunications networks [20], [21], [22], [23].

To the best of our knowledge, a mathematical framework for designing robust coupling interfaces between interdependent critical infrastructures is missing.

C. Contribution

We propose a novel optimization-based mathematical model for the optimal design of coupling interface between interdependent critical infrastructures. The proposed approach ensures the robustness of the coupling interface in terms of worst-case realization of combined performed of the interdependent infrastructures. The proposed approach is based on the DAD model, a three-stage sequential game which allows to identify robust defense strategies and/or resource allocation against a defined set of feasible attack scenarios. Using as an illustrative case-study interdependent power and gas networks (IPGNs), our model ensures a coupling interface design which minimizes the negative consequences, in terms of loss of combined performance within the interdependent CIs, of the worst-case feasible attack scenario.

The contributions of this papers can be summarized as follows:

- We developed a novel and original application of optimization-based design, which can be directly applied in real-world situations such as: *(i)* design of the coupling interface between new CIs, *(ii)* design of the coupling interface between new and existing CIs, *(iii)* analysis and evaluation of existing coupling interfaces.
- We developed a reliable and efficient solution approach, by adapting the Nested Column&Constraint Generation algorithm to our model.
- Using IPGNs as a case-study, we showed that our approach outperform network metrics-based coupling interfaces available in the existing literature.

The rest of this work is organized as follows: in Section II, the problem is formulated; in Section III, the solution procedure is detailed; in Section IV, the case-study is presented in details; in Section V, the main results are reported and discussed; in Section VI, some final remarks and possible future developments are given.

II. Optimization problem formulation

A. Modeling framework

Critical infrastructures are interdependent if the functionality of one system affects the functionality of other connected systems. Relationships of various nature can exist between elements of different infrastructures, and the interdependencies can be divided into four categories: physical, when the state of one system is dependent on the material output of another system; cyber, when the state of one system is dependent on the information transmitted through another system; geographic, when different systems share the same location and their state can be modified by an environmental event; and logical, if the interdependency is not physical, cyber, or geographic [4].

We model each infrastructure using a network flow-based approach [2]. A network is a mathematical construct described by a graph $G = (V, E)$, where V is the set of N nodes and E is the set of M edges. Each edge k is defined by a tuple (i, j), where i and j represent, respectively, the origin node $O(k)$ and destination node $D(k)$ of the corresponding edge. We assume that each node i is characterized by a production capacity $\overline{p}_i$ (e.g. power or gas flow production) and a requested demand $\overline{d}_i$ (e.g. power or gas flow demand). Similarly, each edge k is defined by a maximum flow capacity $\overline{f}_k$.

In the context of K interdependent infrastructures, the focus of our analysis is the combined performance P_C [13], as generally defined in (1):

$$P_C = \sum_{k \in K} w_k \frac{\sum_{i \in V_k} d_i}{\sum_{i \in V_k} \overline{d}_i} \tag{1}$$

where w_k represents the weight of infrastructure k, V_k represents the set of nodes in infrastructure k and d_i represents the demand supplied at node i. This equation represents the fraction of requested demand that is possible to satisfy within the system of interdependent infrastructures.

In this work, we consider interdependent power and gas networks, which are mutually interdependent from each other with physical interdependencies: equipment in the gas network needs to receive electricity, while gas-fired power plants needs a gas flow supply. The power network operations are simulated with a DC power flow model, while the gas network operations are simulated with a maximum flow model, which is a suitable approximation of flow-based infrastructures [24], [13], [25], [26].

Several works analyze critical infrastructures in the context of specific types of hazards, like intentional attacks [25], spatially-localized attacks [14] and extreme natural events [13], [27]. In this work, we adopt an approach based on the maximum number of contingencies [28], [29]. For simplicity, but without loss of generality, we assume that only transmission lines (edges) in the power network can be attacked and failed. We thus adopt the traditional $N - k$ contingencies approach, applied to a interdependent CIs scenario.

B. Tri-level optimization

The problem takes the form of a tri-level defender-attacker-defender (DAD) optimization model, a formulation often used in the framework of optimization of defense strategies and resources in CIs (see e.g. [12], [13], [28]). It is useful to imagine the problem as a three-players game: the inner defender aims at maximizing the combined performance of the IPGN through the operational variables of the two systems; the middle attacker aims at minimizing the combined performance choosing the most disruptive attack plan; the outer defender aims at maximizing the combined performance of the IPGN

by designing a robust coupling interface that also ensures satisfactory performance in nominal conditions. For clarity, with the exception of the most relevant constraints, we report the problem in its compact matrix formulation. The full formulation of the problem is available in Appendix B, with the nomenclature in Appendix A. The problem takes the tri-level formulation shown in (2)-(9).

$$\max_{\substack{\{\mathbf{h^0},\boldsymbol{\delta^0}\}\\ \mathbf{y}\in\{0,1\}^{M_c}}} \min_{\mathbf{u}\in\{0,1\}^{M_A}} \max_{\{\mathbf{h},\boldsymbol{\delta}\}} \mathbf{b}^T\mathbf{h} \tag{2}$$

subject to:

$$\sum_{j\in V_{PN}} y^1_{ij} \leq 1, \quad \forall i \in V_{GN} \tag{3}$$

$$\sum_{j\in V_{GN}} y^2_{ij} \leq 1, \quad \forall i \in V_{PN} \tag{4}$$

$$\sum_{\substack{i\in V_{GN}\\ j\in V_{PN}}} y^1_{ij}\, d^{km}_{ij}\, c^1_{km} + \sum_{\substack{i\in V_{PN}\\ j\in V_{GN}}} y^2_{ij}\, d^{km}_{ij}\, c^2_{km} \leq B_{ci} \tag{5}$$

$$\mathbf{R^0 h^0} \leq \mathbf{q^0} - \mathbf{H^0 y} - \mathbf{W^0}\boldsymbol{\delta^0} - \mathbf{D^0 y}\boldsymbol{\delta^0} \tag{6}$$

$$\mathbf{b}^T\mathbf{h^0} \geq 1 \tag{7}$$

$$\sum_{k\in E_{PN}} (1-u_k) \leq K_{att} \tag{8}$$

$$\mathbf{Rh} \leq \mathbf{q} - \mathbf{Tu} - \mathbf{Hy} - \mathbf{W}\boldsymbol{\delta} - \mathbf{Dy}\boldsymbol{\delta} \tag{9}$$

The variables $\mathbf{h^0}$=$\{\mathbf{p^0}, \mathbf{d^0}, \mathbf{f^0}, \boldsymbol{\theta^0}\}$ and $\boldsymbol{\delta^0}$ are the continuous and binary operational variables of the first stage, and they represent production levels, supplied demands, network flows, voltage angles (in power network nodes) and interdependencies status, respectively; the variables $\mathbf{y}$ are the coupling interface binary variables, and they define how the two infrastructures are coupled to and interdependent on each other. The term M_c denotes the dimension of the vector containing all the feasible combinations of the binary variables $\mathbf{y}$.

The variables $\mathbf{u}$ represents the binary attack variables, and they indicate which power lines are targeted and destroyed by the attacker. The term M_A denotes the dimension of the vector containing all the feasible combinations of the binary variables $\mathbf{u}$.

The variables $\mathbf{h}$=$\{\mathbf{p}, \mathbf{d}, \mathbf{f}, \boldsymbol{\theta}\}$ and $\boldsymbol{\delta}$ denote the continuous and binary operational variables, respectively, of the third stage.

The objective function in (2) represents the fraction of requested demand of gas and electricity which is possible to supply, and its full formulation is shown in (38) in Appendix B.

In the first stage, a defender aims at maximizing the objective function by setting the coupling interface between the power and gas network through the binary variables $\mathbf{y}$=$\{y^1_{ij}, y^2_{ij}\}$, knowing that the following player, the attacker, will aim at minimizing the objective function. The variable y^1_{ij} equals to 1 if the node $i \in V_{GN}$ is coupled to and dependent on the node $j \in V_{PN}$, and 0 otherwise; similarly, the binary variable y^2_{ij} equals to 1 if the node $i \in V_{PN}$ is coupled to and dependent on the node $j \in V_{GN}$, and 0 otherwise. We assume that each node in the gas network that needs electricity is dependent on one and only one node in the power network, as shown in constraint (3); similarly, each node in the power network that requires gas flow supply is dependent on one and only one node in the gas network, as shown in constraint (4). Coupling two nodes has a cost per kilometer, and the total cost of the allocated interdependencies is bounded by the available monetary budget B_{ci}. This is expressed in constraint (5), where d^{km}_{ij} is the distance in km between nodes i and j and the terms c^1_{km} and c^2_{km} are, respectively, the cost per km of placing a coupling link from the power to the gas network and from the gas to the power network.

The coupling interface must be allocated in a way such that, in nominal conditions (no component attacked nor failed), the requested demands of electricity and gas are fully satisfied. This condition is enforced by constraint (7), corresponding to constraint (57) in Appendix B, which depends on the operational constraints of the IPGNs, expressed in constraint (6) and corresponding to constraints (44)-(56) in Appendix B.

In the second stage, an attacker aims at minimizing the combined performance of the IPGNs by failing transmission lines in the power network through the variables $\mathbf{u}$. The variable u_k takes the value 0 if the power line k fails; otherwise it takes the value 1. We assume that the attacker can target a maximum number of lines, as expressed in constraint (8).

In the third stage, a defender aims at maximizing the combined performance of the disrupted IPGNs through the operational variables $\mathbf{h}$ and $\boldsymbol{\delta}$, as expressed in constraint (9), which corresponds to constraints (61)-(76) in Appendix B.

The constraint sets in (6) and (9) represents the operational model of the IPGNs, in nominal conditions and in the contingency scenario $\mathbf{u}$, respectively. The power network is modeled with a DC power flow model, while the gas network is modeled with a maximum flow model, which represents a suitable approximation for flow-based infrastructures [13], [24]. The constraints of these models are shown in Appendix B. Here, it is of particular relevance to illustrate in details the constraints related to the interdependencies and the coupling interface between power and gas network, shown in (10)-(18).

$$0 \leq d_i \leq \overline{d}^b_i + \sum_{j\in V_{GN}} y^1_{ji}\, \overline{d}^{MW}_j, \quad \forall i \in V_{PN} \tag{10}$$

$$0 \leq d_i \leq \overline{d}^b_i + \sum_{j\in V_{PN}} y^2_{ji}\, \overline{d}^{m^3}_j, \quad \forall i \in V_{GN} \tag{11}$$

$$d_i - \delta^{PN}_i \left(\overline{d}^b_i + \sum_{j\in V_{GN}} y^1_{ji}\, \overline{d}^{MW}_j\right) \geq 0, \quad \forall i \in V_{PN} \tag{12}$$

$$d_i - \delta^{GN}_i \left(\overline{d}^b_i + \sum_{j\in V_{PN}} y^2_{ji}\, \overline{d}^{m^3}_j\right) \geq 0, \quad \forall i \in V_{GN} \tag{13}$$

$$p_i - \overline{p}_i \sum_{j \in V_{GN}} y^2_{ij}\, \delta^{GN}_j \leq 0, \quad \forall i \in V_{PN} \tag{14}$$

$$p_i - \overline{p}_i \sum_{j \in V_{PN}} y^1_{ij}\, \delta^{PN}_j \leq 0, \quad \forall i \in V_{GN} \tag{15}$$

$$d_i - \overline{d}^b_i \sum_{j \in V_{PN}} y^1_{ij}\, \delta^{PN}_j - \sum_{j \in V_{PN}} y^2_{ji}\, \overline{d}^{m^3}_j \sum_{j \in V_{PN}} y^1_{ij}\, \delta^{PN}_j \leq 0, \quad \forall i \in V_{GN} \tag{16}$$

$$-\sum_{\substack{i=O(k)\\ j \in V_{PN}}} y^1_{ij}\, \delta^{PN}_i\, \overline{f}_k \leq f_k \leq \sum_{\substack{i=O(k)\\ j \in V_{PN}}} y^1_{ij}\, \delta^{PN}_i\, \overline{f}_k, \quad \forall k \in E_{GN} \tag{17}$$

$$-\sum_{\substack{i=D(k)\\ j \in V_{PN}}} y^1_{ij}\, \delta^{PN}_i\, \overline{f}_k \leq f_k \leq \sum_{\substack{i=D(k)\\ j \in V_{PN}}} y^1_{ij}\, \delta^{PN}_i\, \overline{f}_k, \quad \forall k \in E_{GN} \tag{18}$$

The supplied demand d_i is bounded between 0 and the requested demand. Contrary to traditional approaches, the requested demand in each node is not a fixed parameter but it depends on the coupling interface, as shown in (10) and (11). The requested demand in each node i, either in the power or gas network, is composed of two terms:

- The term $\overline{d}^b_i$ is the base requested demand, which represent various consumers of electricity/gas (households, industries, etc.).
- The second term, $\sum_{j \in V_{GN}} y^1_{ji}\, \overline{d}^{MW}_j$ in (10) and $\sum_{j \in V_{PN}} y^2_{ji}\, \overline{d}^{m^3}_j$ in (11), represents the electricity/gas demand of all the nodes of the other infrastructures dependent on the node i. The terms $\overline{d}^{MW}_j$ and $\overline{d}^{m^3}_j$ represent, respectively, the electricity demand of node $j \in V_{GN}$ and the gas flow demand of node $j \in V_{PN}$.

The status of each interdependency is described in (12) and (13). Each interdependency from the node $i \in V_{PN}$ to the node $j \in V_{GN}$ is functional if the variable δ^{PN}_i is equal to 1; otherwise, δ^{PN}_i=0 and the interdependency is not functional. We assume, as shown in (12), that each variable δ^{PN}_i can take the value 1 only when the requested demand in the node i is fully supplied. The same assumption is applied for the gas network and the corresponding variables δ^{GN}_i, as shown in (13).

The production level p_i in each node depends on the coupling interface. We assume that the production p_i in each node ranges between 0 and the production capacity $\overline{p}_i$ if there is one functional interdependency, and 0 otherwise. For example, as shown in (14), the production p_i in the node $i \in V_{PN}$ ranges between 0 and $\overline{p}_i$ if there is one interdependency from a node $j \in V_{GN}$ in the gas network (y^2_{ij}=1) properly functional (δ^{GN}_j=1); otherwise, p_i takes the value 0. The same assumption is applied for the gas network and the corresponding interdependency from the power network, as shown in (15). In addition, we assume that, in the gas network, supplied demands and flows in the pipes are also dependent on the interdependency from the power network. As shown in (16), the supplied demand d_i in the node $i \in V_{GN}$ ranges between 0 and the requested demand if there is one interdependency from a node $j \in V_{PN}$ in the power network (y^1_{ij}=1) properly functional (δ^{PN}_j=1); otherwise, d_i takes the value 0. Lastly, we assume that the absolute value of the flow f_k in each pipe $k \in E_{GN}$ ranges between 0 and the maximum flow capacity $\overline{f}_k$ only if both the origin and destination node of k, respectively $O(k)$ and $D(k)$, have a functional interdependency from the power network, as expressed in (17) and (18); otherwise, f_k takes the value 0.

The constraints in (10)-(18) are nonlinear due to the multiplication of variables $\boldsymbol{\delta}$ and $\mathbf{y}$. These terms can be linearized by introducing new binary variables $\mathbf{z}$ and $\mathbf{r}$. The full linearization is reported in Appendix C. The problem can, thus, be expressed as a tri-level mixed-integer linear program (MILP), as shown in the compact formulation (19)-(21).

$$\max_{\substack{\{\mathbf{h^0},\boldsymbol{\delta^0}\}\\ \mathbf{y} \in \{0,1\}^{M_c}}} \; \min_{\mathbf{u} \in \{0,1\}^{M_A}} \; \max_{\{\mathbf{h},\boldsymbol{\delta}\}} \mathbf{b}^T\mathbf{h} \tag{19}$$

subject to (3)-(5), (7)-(8) and (20)-(21):

$$\mathbf{R^0 h^0} \leq \mathbf{q^0} - \mathbf{H^0 y} - \mathbf{W^0 \delta^0} - \mathbf{S^0 z^0} - \mathbf{V^0 r^0} \tag{20}$$

$$\mathbf{Rh} \leq \mathbf{q} - \mathbf{Tu} - \mathbf{Hy} - \mathbf{W\delta} - \mathbf{Sz} - \mathbf{Vr} \tag{21}$$

III. Solution procedure

The presence of the binary variables $\boldsymbol{\delta}$ in the third stage makes it impossible to merge the second and third stage into a single min problem relying on the strong duality (or Karush-Kuhn-Tucker) reformulation. We thus adopt a cutting plane strategy, called Nested Column&Constraint Generation (NC&CG) algorithm, originally developed for solving robust optimization problems. It represents an exact method, with proven convergence to the global optimum, for solving multi-level mixed-integer linear programming with recourse problems [30], [31].

The flowchart of the algorithm is shown in Figure 1. In order to adopt this strategy, the original tri-level max-min-max problem must be expanded into a max-min-max-max problem, separating binary and continuous variables in the original third stage. The new fourth stage contains only continuous variables, and it is then a pure LP problem. The formulation is then transformed into a max-min-max-min through a dual reformulation of the last stage. In this form, the problem can be solved using a NC&CG algorithm, identifying an outer and inner layer which exchange primal variables in form of parameters until the convergence to the global optimum is reached.

To simplify the following explanation we rely on a compact formulation. For a more detailed explanation of the C&CG algorithm, the reader is referred to [30], [31] for a theoretical framework and [13], [28], [29] for applications.

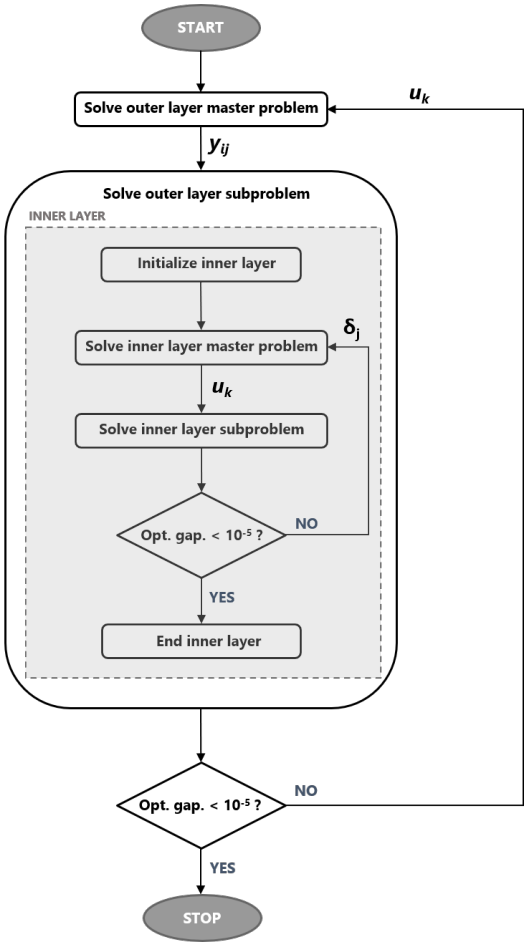

Fig. 1: Flowchart of the NC&CG algorithm.

A. Inner layer

The inner layer consists in the solution of the second and third stage (min-max) in (19) for a fixed coupling interface $\mathbf{y}^*$. The output of the model is the worst-case realization of the combined performance and the associated optimal attack plan $\widehat{\mathbf{u}}$. For a fixed coupling interface $\mathbf{y}^*$, fixed interdependency variables $\boldsymbol{\delta}^*$ and fixed attack plan $\mathbf{u}^*$, the compact form of the inner-most maximization in (19) and the relative constraints are shown in (22)-(23):

$$\max_{\mathbf{h}} \mathbf{b}^T\mathbf{h} \tag{22}$$

subject to :

$$\mathbf{Rh} \leq \mathbf{q} - \mathbf{Tu}^* - \mathbf{Hy}^* - \mathbf{W}\boldsymbol{\delta}^* - \mathbf{Dy}^*\boldsymbol{\delta}^* \tag{23}$$

The problem in (22)-(23) is a pure LP, and thus the introduction of variables $\mathbf{z}$ and $\mathbf{r}$ is not necessary. Its dual form is expressed in (24)-(25):

$$\min_{\boldsymbol{\lambda}} (\mathbf{q} - \mathbf{Tu}^* - \mathbf{Hy}^* - \mathbf{W}\boldsymbol{\delta}^* - \mathbf{Dy}^*\boldsymbol{\delta}^*)^T\boldsymbol{\lambda} \tag{24}$$

subject to:

$$\mathbf{R}^T\boldsymbol{\lambda} = \mathbf{b} \tag{25}$$

From the above formulation, we can proceed to solve the inner layer problem using the C&CG algorithm. This is achieved by employing a partial set of feasible interdependency variables combinations $\mathcal{D}_{part} \subseteq \mathcal{D}$, and proceeding as expressed in the following steps:

1) Set $h = 0$, upper bound $UB_{in} = \infty$, lower bound $LB_{in} = 0$ and $\mathcal{D}_{part} = \emptyset$
2) Solve the inner master problem in Equations (26)-(29). Obtain an optimal solution $\widehat{\rho}^{(h)}$ and $\widehat{\mathbf{u}}^{(h)}$. Update LB_{in}=$\widehat{\rho}^{(h)}$.

$$\min_{\{\rho,\mathbf{u},\boldsymbol{\lambda}\}} \rho \tag{26}$$

subject to:

$$\rho \geq (\mathbf{q} - \mathbf{Tu} - \mathbf{Hy}^* - \mathbf{W}\boldsymbol{\delta}^{*(h)} - \mathbf{Dy}^*\boldsymbol{\delta}^{*(h)})^T\boldsymbol{\lambda}^{(h)}, \quad \forall\boldsymbol{\delta}^{*(h)} \in \mathcal{D}_{part} \tag{27}$$

$$\mathbf{R}^T\boldsymbol{\lambda}^{(h)} = \mathbf{b}, \quad \forall\boldsymbol{\delta}^{*(h)} \in \mathcal{D}_{part} \tag{28}$$

$$\sum_{k\in E_{PN}} (1 - u_k) \leq K_{att} \tag{29}$$

3) Solve the inner subproblem in Equations (30)-(31) with $\widehat{\mathbf{u}}^{(h)}$=$\mathbf{u}^*$. Obtain an optimal solution $\mathbf{b}^T\widehat{\mathbf{h}}^{(h)}$ and $\widehat{\boldsymbol{\delta}}^{(h)}$. Set $UB_{in} = \min(UB_{in}, \mathbf{b}^T\widehat{\mathbf{h}}^{(h)})$.

$$\max_{\{\mathbf{h},\boldsymbol{\delta}\}} \mathbf{b}^T\mathbf{h} \tag{30}$$

subject to :

$$\mathbf{Rh} \leq \mathbf{q} - \mathbf{Tu}^* - \mathbf{Hy}^* - \mathbf{W}\boldsymbol{\delta} - \mathbf{Dy}^*\boldsymbol{\delta} \tag{31}$$

4) If $(UB_{in} - LB_{in})/UB_{in} < 10^{-5}$, the current solution $\widehat{\mathbf{u}}^{(h)}$ corresponds to the optimal attack and the algorithm can be terminated. Otherwise, $\mathcal{D}_{part} = \mathcal{D}_{part} \cup \widehat{\boldsymbol{\delta}}^{(h)}$. Set $h \leftarrow h + 1$ and return to step 2.

This algorithm corresponds to the inner layer in Figure 1. Its output is the optimal attack plan, or, in other words, the feasible combination of variables $\mathbf{u}$ which minimizes the combined performance for a fixed coupling interface $\mathbf{y}^*$.

B. Outer layer

The outer layer can be solved in a similar way, by employing a partial set of feasible attack scenarios $\mathcal{A}_{part} \subseteq \mathcal{A}$. While the inner layer solves a bi-level min-max problem, the outer layer solves a bi-level max-min problem, where the minimization represents the outer subproblem, and it is solved by the inner layer in the previous section.

Similar to the inner layer, the outer layer is solved with a C&CG algorithm with the following steps:

1) Set $h = 0$, upper bound $UB_{out} = \infty$, lower bound $LB_{out} = 0$ and $\mathcal{A}_{part} = \emptyset$
2) Solve the outer master problem in Equations (32)-(37). Obtain an optimal solution $\widehat{\eta}^{(h)}$ and $\widehat{\mathbf{y}}^{(h)}$. Update UB_{out}=$\min(UB_{out}, \widehat{\eta}^{(h)})$

$$\max_{\substack{\{\eta,\mathbf{h}^{(h)}\} \\ \{\mathbf{h}^{\mathbf{0}},\boldsymbol{\delta}^{\mathbf{0}}\} \\ \mathbf{y}\in\{0,1\}^{M_c}}} \eta \tag{32}$$

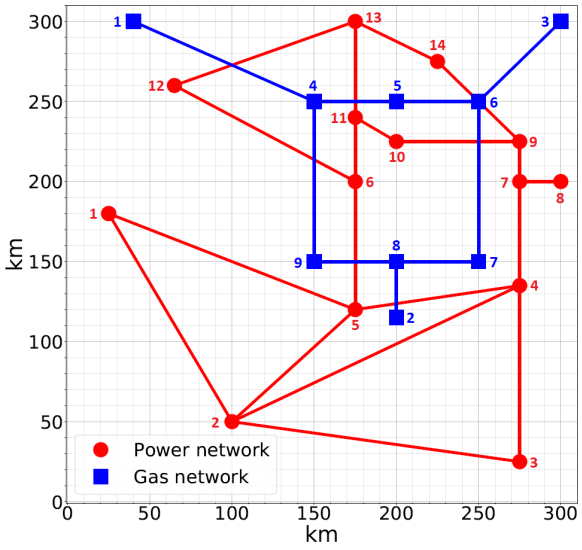

Fig. 2: Geographical allocation of the interdependent power and gas network.

$$\eta \leq \mathbf{b}^T \mathbf{h}^{(h)}, \quad \forall \mathbf{u}^{*(h)} \in \mathcal{A}_{part} \tag{33}$$

$$\mathbf{P}_{out}\mathbf{y} \leq \mathbf{g}_{out} \tag{34}$$

$$\mathbf{R}^0\mathbf{h}^0 \leq \mathbf{q}^0 - \mathbf{H}^0\mathbf{y} - \mathbf{W}^0\boldsymbol{\delta}^0 - \mathbf{S}^0\mathbf{z}^0 - \mathbf{V}^0\mathbf{r}^0 \tag{35}$$

$$\mathbf{b}^T\mathbf{h}^0 \geq 1 \tag{36}$$

$$\begin{aligned}\mathbf{R}\mathbf{h}^{(h)} \leq \mathbf{q} - \mathbf{T}\mathbf{u}^{*(h)} - \mathbf{H}\mathbf{y} - \mathbf{W}\boldsymbol{\delta}^{(h)} \\ -\mathbf{S}\mathbf{z}^{(h)} - \mathbf{V}\mathbf{r}^{(h)}, \ \forall \mathbf{u}^{*(h)} \in \mathcal{A}_{part}\end{aligned} \tag{37}$$

where $\mathbf{P}_{out}$ and $\mathbf{g}_{out}$ are the coefficient matrix and the parameter vector of constraints in (3)-(5).

3) Solve the outer subproblem using the inner C&CG algorithm explained in the previous subsection with $\widehat{\mathbf{y}}^{(h)}$=$\mathbf{y}^*$. Obtain an optimal solution $\mathbf{b}^T\widehat{\mathbf{h}}^{(h)}$ and an optimal attack plan $\widehat{\mathbf{u}}^{(h)}$. Set $LB_{out} = \mathbf{b}^T\widehat{\mathbf{h}}^{(h)}$.
4) If $(UB_{out} - LB_{out})/UB_{out} < 10^{-5}$, the current solution $\widehat{\mathbf{y}}^{(h)}$ corresponds to the optimal coupling interface and the algorithm can be terminated. Otherwise, $\mathcal{A}_{part} = \mathcal{A}_{part} \cup \widehat{\mathbf{u}}^{(h)}$. Set $h \leftarrow h+1$ and return to step 2.

The output represents the optimal coupling interface which maximizes the worst realization of the IPGNs combined performance under external attacks.

IV. Case-study

As an illustrative example, we consider a power network with a topology based on the IEEE 14-bus system, and a gas network with a topology based on the IEEE 9-bus system. We assume that the two infrastructures are placed within a 300×300 km^2 geographical area, as shown in Figure 2. Each infrastructure is assumed to have a weight, respectively w_{PN} and w_{GN}, equal to 0.5. This value represents the importance of each infrastructure when computing the combined performance. Other parameters are available in Appendix D.

TABLE I: Cost of network metrics-based coupling interfaces.

Interface	Cost
DD_{ast}	1953$
DD_{dst}	2201$
BB_{ast}	1757$
BB_{dst}	2080$
Euclidean	823$

We test our model for values of K_{att} ranging from 1 to 5. We choose a representative interdependency cost-per-kilometer of 1 $/km, for both c^1_{km} and c^2_{km}. We assume budget values B_{ci} ranging from 900$ to 1500$ for the installment of coupling interfaces. We compare the results obtained by our model with the results obtained with network metrics-based coupling interfaces, which are identified based on different combinations of node degree (D) and betweenness (B). We distinguish four coupling interfaces using the different network metrics and the terms *assortative* (subscript ast) and *disassortative* (subscript dst). In network science, the assortativity (disassortativity) is a property that describes the tendency of the nodes of a network to be connected to nodes which are similar (different) regarding some specific properties [32]. For example, it can refer to the tendency of high degree nodes to be attached to other high degree nodes. Additionally, we identify a geographical location-based coupling interface, referred to as *Euclidean*. The five different network metrics-based interfaces used in this work are characterized by the following features:

- DD_{ast}: the node with the k^{th} highest degree in the power network (or gas network) is dependent on the node with the k^{th} highest degree in the gas network (or power network).
- DD_{dst}: the node with the k^{th} highest degree in the power network (or gas network) is dependent on the node with the k^{th} lowest degree in the gas network (or power network).
- BB_{ast}:the node with the k^{th} highest betweenness in the power network (or gas network) is dependent on the node with the k^{th} highest betweenness in the gas network (or power network).
- BB_{dst}: the node with the k^{th} highest betweenness in the power network (or gas network) is dependent on the node with the k^{th} lowest betweenness in the gas network (or power network).
- Euclidean: each node in the power network (or gas network) is dependent on the geographically closest node in the gas network (or power network).

The cost associated with each network metrics-based coupling interface is reported in Table I.

Finally, all the computations are implemented in the Python API of Gurobi 9.1 [33] and performed on a laptop with a 2.60 GHz CPU and 16 GB RAM.

V. RESULTS

A. Combined performance

The results for the network metrics-based coupling interfaces are shown in Figure 3a, while the results for the optimal coupling interfaces obtained by our approach with different budget B_{ci} are shown in Figure 3b. The x-axis shows the maximum number of lines in the power network which can be attacked and failed; the y-axis shows the correspondent worst-case realization of the combined performance. The conservativeness of the model can be tuned using the maximum number of failed lines K_{att}.

The two sets of coupling interfaces are designed, by default, with different assumptions:

- The network metrics-based coupling interfaces are designed using network properties as guidelines for coupling nodes of different infrastructures. This approach is already described in the existing literature. The associated costs in Table I are shown merely for comparison with our approach, and they do not affect the design of the network metrics-based coupling interfaces.
- The proposed approach provides the most robust coupling interface for a given monetary budget. In this case, the cost of the coupling interface allocation is key parameter of the model.

The main comparison metric is the worst-case combined performance within the different cases. The purpose of our analysis is to show that the proposed approach outperforms the network metrics-based coupling interfaces, leading, *de facto*, to the most robust coupling interface for a given monetary budget.

As it can be clearly seen in Figure 3a, the disassortative interfaces (DD_{dst} and BB_{dst}) perform poorly, as the worst-case combined performance decreases rapidly with the increasing of the attack budget K_{att}, reaching the value 0 for K_{att}=4. The assortative interfaces, especially BB_{ast}, perform better, as the related worst-case combined performance is higher than the disassortative interfaces with the increasing K_{att}. Particularly, for BB_{ast}, with K_{att}=4 and K_{att}=5, the worst-case combined performance are 0.49 and 0.29, respectively, while for the disassortative interfaces the performance in both cases is 0.

The Euclidean coupling interface leads to even better performance than BB_{ast}: for K_{att}=3, K_{att}=4 and K_{att}=5, the BB_{ast} interface leads to worst-case combined performance respectively of 0.60, 0.49 and 0.29, while the Euclidean interface leads respectively to 0.70, 0.52 and 0.31.

These results clearly show how different coupling interfaces lead to different worst-case combined performance. In this case, the Euclidean coupling interface performs better than the other network metrics-based coupling interfaces. However, these results should not be generalized, as the performance of each network metrics-based coupling interface is strongly case-dependent. For example, if we change the geographical disposition of the nodes of the IPGN, the Euclidean coupling interface would be different and, thus, the results would differ. Similar considerations are valid for the other network metrics-based coupling interfaces.

The optimal coupling interfaces, identified with the proposed optimization model, outperform the network metrics-based coupling patterns in terms of worst-case combined performance, as it can be clearly seen in Figure 3b. The minimum budget which ensures the feasibility of the model is 823$, which corresponds to the cost of the Euclidean coupling interface, which is based on the minimum geographical distance. For a budget lower than 823$ it is not possible to allocate all the necessary interdependencies and thus ensure satisfactory performance in nominal conditions. The results for B_{ci}=823$ (blue triangles in Figure 3b) are thus equivalent to the results of the Euclidean coupling interface (blue triangles in Figure 3a).

As it can be clearly seen, for values of B_{ci} greater than 823$, the traditional interfaces are outperformed by the optimal coupling interfaces identified by the proposed approach. For example, with B_{ci}=900$ and K_{att}=3, K_{att}=4 and K_{att}=5, the worst-case combined performance are respectively 0.77, 0.64 and 0.51. These results are considerably higher than the previously explained Euclidean interface.

The worst-case combined performance improves with the increasing of the budget B_{ci}. For example, with B_{ci}=1500$ and K_{att}=3, K_{att}=4 and K_{att}=5, the worst-case combined performance are respectively 0.93, 0.91 and 0.86. For values of B_{ci} greater than 1500$, the results do not improve. The case B_{ci}=1500$ (pink triangles in Figure 3b) leads to the best possible results for this case-study.

B. Computational cost

The computational time in seconds of the NC&CG algorithm is shown in Table II. In this study, the computational cost is acceptable, as the longest instance of the NC&CG algorithm occurs for B_{ci}=900$ and K_{att}=4, and it takes 525 seconds.

For larger case-studies, the computational time might increase considerably, due to the large number of binary variables involved. However, an increased computational cost does not represent an insurmountable issue: firstly, this model is tailored to be utilized during design phases, and long computational times do not pose particular problems; secondly, the complexity of the model can be reduced limiting the feasible number of coupling interfaces according to geographical and physical constraints. For example, one can assume that only nodes within a specific distance range can be coupled together (e.g. only nodes within 100 km from each other); this would limit the number of $\mathbf{y}$ variables involved, thus reducing the complexity and computational cost of the model.

VI. CONCLUSION

In this paper, we have proposed a novel mathematical programming framework for the identification of the optimal coupling interface between interdependent critical infrastructures, using as an illustrative case-study interdependent power and gas networks. The proposed approach outperformed network metrics-based approaches utilized in the existing literature, and the identified solutions represent the most robust coupling interfaces under different feasible attacks sets and monetary budget.

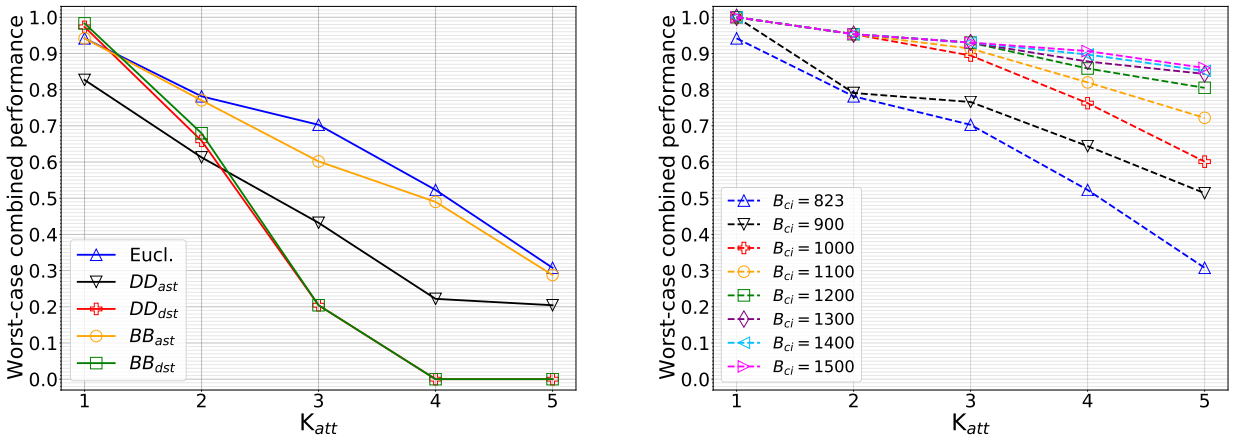

(a) Network-based coupling interfaces

(b) Optimal coupling interfaces

Fig. 3: Simulation results for the network.

TABLE II: Computational time in seconds of the NC&CG algorithm.

B_{ci}	K_{att}=1	K_{att}=2	K_{att}=3	K_{att}=4	K_{att}=5
823	2.54	9.40	18.76	70.68	109.03
900	6.33	14.69	35.56	525.34	287.17
1000	3.60	18.24	24.72	168.52	353.26
1100	2.19	11.54	85.51	128.61	407.48
1200	8.12	27.88	28.61	204.97	77.39
1300	9.44	22.08	34.94	71.06	74.89
1400	6.02	25.02	74.17	49.97	74.89
1500	2.04	19.21	46.07	27.62	53.79

In summary, the contributions of this paper are:

- The development of a novel approach for the robust design of coupling interfaces.
- The development of a reliable and efficient solution procedure based on the Nested Column&Constraint Generation algorithm.
- The development of a case-study to show that the proposed approach outperforms network metrics-based coupling interface designs and lead to the most robust solution.

The proposed case-study is based on interdependent power and gas networks, modeled using a DC power flow model and a maximum flow model, respectively. However, the proposed approach can be applied to any combination of interdependent critical infrastructures.

The proposed approach outperforms other coupling strategies in terms of robustness against external attacks, as it allows identifying the most robust coupling interface. The conservativeness of the model can be tuned adjusting the size of the feasible attacks set, with variations of maximum number of lines attacked and failed. The model can be easily adapted to different disruption scenarios, for example including failure of nodes.

Our solution strategy leads to acceptable computational times in this work. However, the computational cost might increase considerably for larger case-studies. Nevertheless, it does not represent a particular issue, since this approach aims at being used during design phases.

Further improvements of this work will consist in the inclusion of failure probabilities within the proposed approach, such to identify robust coupling interfaces under uncertain disruption scenarios.

Appendix A
Nomenclature

Sets

V_{PN}	Set of nodes in the power network.
E_{PN}	Set of edges in the power network.
V_{GN}	Set of nodes in the gas network.
E_{GN}	Set of edges in the gas network.
V_{TOT}	Set of nodes $V_{PN} \cup V_{GN}$.
E_{TOT}	Set of edges $E_{PN} \cup E_{GN}$.

Variables first stage

$\mathbf{y}$	Vector of coupling interface variables y^1_{ij} and y^2_{ij}.
$\mathbf{p^0}$	Vector of production variables p^0_i.
$\mathbf{d^0}$	Vector of demand variables d^0_i.
$\mathbf{f^0}$	Vector of flow variables f^0_k.
$\boldsymbol{\theta^0}$	Vector of phase angle variables θ^0_k.
$\boldsymbol{\delta^0}$	Vector of interdependency variables $\delta^{PN,0}_i$ and $\delta^{GN,0}_i$.
y^1_{ij}	Binary coupling variable between nodes $i \in V_{GN}$ and $j \in V_{PN}$.
y^2_{ij}	Binary coupling variable between nodes $i \in V_{PN}$ and $j \in V_{GN}$.
p^0_i	Production variable at node i.
d^0_i	Demand variable at node i.
f^0_k	Flow variable at edge k.
θ^0_k	Phase angle variable at node $i \in V_{PN}$.
$\delta^{PN,0}_i$	Binary interdependency state variable at node $i \in V_{PN}$.
$\delta^{GN,0}_i$	Binary interdependency state variable at node $i \in V_{GN}$.

Variables second stage

$\mathbf{u}$	Vector of attack variables u_k.
u_k	Binary attack variable at edge $k \in E_{PN}$.

Variables third stage

$\mathbf{p}$	Vector of production variables p_i.
$\mathbf{d}$	Vector of demand variables d_i.
$\mathbf{f}$	Vector of flow variables f_k.
$\boldsymbol{\theta}$	Vector of phase angle variables θ_k.
$\boldsymbol{\delta}$	Vector of interdependency variables δ_i^{PN} and δ_i^{GN}.
p_i	Production variable at node i.
d_i	Demand variable at node i.
f_k	Flow variable at edge k.
θ_k	Phase angle variable at node $i \in V_{PN}$.
δ_i^{PN}	Binary interdependency state variable at node $i \in V_{PN}$.
δ_i^{GN}	Binary interdependency state variable at node $i \in V_{GN}$.

Other variables

$\mathbf{z}$	Vector of variables z_{ij}^1 and z_{ij}^2.
$\mathbf{r}$	Vector of attack variables r_{ij}.
z_{ij}^1	Binary variable for linearizing quadratic terms in the first and third stage.
z_{ij}^2	Binary variable for linearizing quadratic terms in the first and third stage.
r_{ij}	Binary variable for linearizing cubic terms in the first and third stage.

Parameters

c_{km}^1	Cost per km of interdependency from power network to gas network.
c_{km}^2	Cost per km of interdependency from gas network to power network.
d_{ij}^{km}	Distance in km between nodes i and j.
B_{ci}	Budget for coupling interface allocation.
$\overline{p}_i$	Production capacity in node i.
$\overline{d}_i^b$	Base requested demand in node i.
$\overline{d}_{PN}^{max}$	Total requested demand in power network.
$\overline{d}_{GN}^{max}$	Total requested demand in gas network.
$\overline{d}_i^{MW}$	Electricity demand of node $i \in V_{GN}$.
$\overline{d}_i^{m^3}$	Gas flow demand of node $i \in V_{PN}$.
$\overline{f}_k$	Flow capacity of edge k.
x_k	Reactance of line k in pu.
w_{PN}	Weight of the power network.
w_{GN}	Weight of the gas network.
K_{att}	Maximum number of edges attacked and failed in the power network.

APPENDIX B
TRI-LEVEL NONLINEAR OPTIMIZATION PROGRAM

$$\max_{\substack{\{\mathbf{p^0},\mathbf{d^0},\mathbf{f^0},\boldsymbol{\theta^0},\boldsymbol{\delta^0}\}\\ \mathbf{y}\in\{0,1\}^{M_c}}} \min_{\mathbf{u}\in\{0,1\}^{M_A}} \max_{\{\mathbf{p},\mathbf{d},\mathbf{f},\boldsymbol{\theta},\boldsymbol{\delta}\}} w_{PN}\frac{\sum_{i\in V_{PN}} d_i}{\overline{d}_{PN}^{max}} + w_{GN}\frac{\sum_{i\in V_{GN}} d_i}{\overline{d}_{GN}^{max}} \quad (38)$$

where $\overline{d}_{PN}^{max}$ and $\overline{d}_{GN}^{max}$ are defined in (39) and (40):

$$\overline{d}_{PN}^{max} = \sum_{i\in V_{PN}} \overline{d}_i^b + \sum_{j\in V_{GN}} \overline{d}_j^{MW} \quad (39)$$

$$\overline{d}_{GN}^{max} = \sum_{i\in V_{GN}} \overline{d}_i^b + \sum_{j\in V_{PN}} \overline{d}_j^{m^3} \quad (40)$$

subject to:

First stage

$$\sum_{j\in V_{PN}} y_{ij}^1 \le 1, \quad \forall i \in V_{GN} \quad (41)$$

$$\sum_{j\in V_{GN}} y_{ij}^2 \le 1, \quad \forall i \in V_{PN} \quad (42)$$

$$\sum_{\substack{i\in V_{GN}\\ j\in V_{PN}}} y_{ij}^1\, d_{ij}^{km}\, C_{km}^1 + \sum_{\substack{i\in V_{PN}\\ j\in V_{GN}}} y_{ij}^2\, d_{ij}^{km}\, C_{km}^2 \le B_{ci} \quad (43)$$

$$0 \le p_i^0 \le \overline{p}_i, \quad \forall i \in V_{TOT} \quad (44)$$

$$0 \le d_i^0 \le \overline{d}_i^b + \sum_{j\in V_{GN}} y_{ji}^1\, \overline{d}_j^{MW}, \quad \forall i \in V_{PN} \quad (45)$$

$$0 \le d_i^0 \le \overline{d}_i^b + \sum_{j\in V_{PN}} y_{ji}^2\, \overline{d}_j^{m^3}, \quad \forall i \in V_{GN} \quad (46)$$

$$-\overline{f}_k \le f_k^0 \le \overline{f}_k, \quad \forall k \in E_{TOT} \quad (47)$$

$$x_k f_k^0 - (\theta_{O(k)}^0 - \theta_{D(k)}^0) = 0, \quad \forall k \in E_{PN} \quad (48)$$

$$p_i^0 - d_i^0 + \sum_{D(k)=i} f_k^0 - \sum_{O(k)=i} f_k^0 = 0, \quad \forall i \in V_{TOT} \quad (49)$$

$$d_i - \delta_i^{PN,0}\Big(\overline{d}_i^b + \sum_{j\in V_{GN}} y_{ji}^1\, \overline{d}_j^{MW}\Big) \ge 0, \quad \forall i \in V_{PN} \quad (50)$$

$$d_i^0 - \delta_i^{GN,0}\Big(\overline{d}_i^b + \sum_{j\in V_{PN}} y_{ji}^2\, \overline{d}_j^{m^3}\Big) \ge 0, \quad \forall i \in V_{GN} \quad (51)$$

$$p_i^0 - \overline{p}_i \sum_{j\in V_{GN}} y_{ij}^2\, \delta_j^{GN,0} \le 0, \quad \forall i \in V_{PN} \quad (52)$$

$$p_i^0 - \overline{p}_i \sum_{j\in V_{PN}} y_{ij}^1\, \delta_j^{PN,0} \le 0, \quad \forall i \in V_{GN} \quad (53)$$

$$d_i - \overline{d}_i^b \sum_{j\in V_{PN}} y_{ij}^1\, \delta_j^{PN} - \sum_{j\in V_{PN}} y_{ji}^2\, \overline{d}_j^{m^3} \sum_{j\in V_{PN}} y_{ij}^1\, \delta_j^{PN} \le 0, \quad \forall i \in V_{GN} \quad (54)$$

$$-\sum_{\substack{i=O(k)\\ j\in V_{PN}}} y^1_{ij}\,\delta^{PN,0}_i\,\overline{f}_k \le f^0_k \le \sum_{\substack{i=O(k)\\ j\in V_{PN}}} y^1_{ij}\,\delta^{PN,0}_i\,\overline{f}_k, \quad \forall k\in E_{GN} \tag{55}$$

$$-\sum_{\substack{i=D(k)\\ j\in V_{PN}}} y^1_{ij}\,\delta^{PN,0}_i\,\overline{f}_k \le f^0_k \le \sum_{\substack{i=D(k)\\ j\in V_{PN}}} y^1_{ij}\,\delta^{PN,0}_i\,\overline{f}_k, \quad \forall k\in E_{GN} \tag{56}$$

$$w_{PN}\frac{\sum_{i\in V_{PN}} d^0_i}{\overline{d}^{max}_{PN}} + w_{GN}\frac{\sum_{i\in V_{GN}} d^0_i}{\overline{d}^{max}_{GN}} \ge 1 \tag{57}$$

$$y_{ij}\in\{0,1\}, \quad \forall i\in V_{GN},\,\forall j\in V_{PN} \tag{58}$$

Second stage

$$\sum_{k\in E_{PN}} (1-u_k) \le K_{att} \tag{59}$$

$$u_k\in\{0,1\}, \quad \forall k\in E_{PN} \tag{60}$$

Third stage

$$0\le p_i\le \overline{p}_i, \quad \forall i\in V_{TOT} \tag{61}$$

$$0\le d_i\le \overline{d}^b_i + \sum_{j\in V_{GN}} y^1_{ji}\,\overline{d}^{MW}_j, \quad \forall i\in V_{PN} \tag{62}$$

$$0\le d_i\le \overline{d}^b_i + \sum_{j\in V_{PN}} y^2_{ji}\,\overline{d}^{m^3}_j, \quad \forall i\in V_{GN} \tag{63}$$

$$-u_k\overline{f}_k \le f_k \le u_k\overline{f}_k, \quad \forall k\in E_{PN} \tag{64}$$

$$-\overline{f}_k \le f_k \le \overline{f}_k, \quad \forall k\in E_{GN} \tag{65}$$

$$x_k f_k - \left(\theta_{O(k)} - \theta_{D(k)}\right) \ge -M_k(1-u_k), \forall k\in E_{PN} \tag{66}$$

$$x_k f_k - \left(\theta_{O(k)} - \theta_{D(k)}\right) \le M_k(1-u_k), \ \ \forall k\in E_{PN} \tag{67}$$

$$p_i - d_i + \sum_{D(k)=i} f_k - \sum_{O(k)=i} f_k = 0, \ \ \forall i\in V_{TOT} \tag{68}$$

$$d_i - \delta^{PN}_i\left(\overline{d}^b_i + \sum_{j\in V_{GN}} y^1_{ji}\,\overline{d}^{MW}_j\right) \ge 0, \quad \forall i\in V_{PN} \tag{69}$$

$$d_i - \delta^{GN}_i\left(\overline{d}^b_i + \sum_{j\in V_{PN}} y^2_{ji}\,\overline{d}^{m^3}_j\right) \ge 0, \quad \forall i\in V_{GN} \tag{70}$$

$$p_i - \overline{p}_i \sum_{j\in V_{GN}} y^2_{ij}\,\delta^{GN}_j \le 0, \quad \forall i\in V_{PN} \tag{71}$$

$$p_i - \overline{p}_i \sum_{j\in V_{PN}} y^1_{ij}\,\delta^{PN}_j \le 0, \quad \forall i\in V_{GN} \tag{72}$$

$$d_i - \overline{d}^b_i \sum_{j\in V_{PN}} y^1_{ij}\,\delta^{PN}_j - \sum_{j\in V_{PN}} y^2_{ji}\,\overline{d}^{m^3}_j \sum_{j\in V_{PN}} y^1_{ij}\,\delta^{PN}_j \le 0, \quad \forall i\in V_{GN} \tag{73}$$

$$-\sum_{\substack{i=O(k)\\ j\in V_{PN}}} y^1_{ij}\,\delta^{PN}_i\,\overline{f}_k \le f_k \le \sum_{\substack{i=O(k)\\ j\in V_{PN}}} y^1_{ij}\,\delta^{PN}_i\,\overline{f}_k, \quad \forall k\in E_{GN} \tag{74}$$

$$-\sum_{\substack{i=D(k)\\ j\in V_{PN}}} y^1_{ij}\,\delta^{PN}_i\,\overline{f}_k \le f_k \le \sum_{\substack{i=D(k)\\ j\in V_{PN}}} y^1_{ij}\,\delta^{PN}_i\,\overline{f}_k, \quad \forall k\in E_{GN} \tag{75}$$

$$\delta^{PN}_i, \delta^{GN}_i \in \{0,1\},\ \theta_j \text{ free},\ \forall i\in V_{TOT}, \forall j\in V_{PN} \tag{76}$$

APPENDIX C
CONSTRAINTS LINEARIZATION

$$d_i - \delta^{PN}_i\overline{d}_i + \sum_{j\in V_{GN}} z^1_{ji}\,\overline{d}^{MW}_j \ge 0, \quad \forall i\in V_{PN} \tag{77}$$

$$d_i - \delta^{GN}_i\overline{d}_i + \sum_{j\in V_{PN}} z^2_{ji}\,\overline{d}^{m^3}_j \ge 0, \quad \forall i\in V_{GN} \tag{78}$$

$$p_i - \overline{p}_i \sum_{j\in V_{GN}} z^2_{ij} \le 0, \quad \forall i\in V_{PN} \tag{79}$$

$$p_i - \overline{p}_i \sum_{j\in V_{PN}} z^1_{ij} \le 0, \quad \forall i\in V_{GN} \tag{80}$$

$$d_i - \overline{d}_i \sum_{j\in V_{PN}} z^1_{ij} - \overline{d}^{m^3}_j \sum_{\substack{i\in V_{PN}\\ k\in V_{PN}}} r_{jik} \le 0, \ \ \forall i\in V_{GN} \tag{81}$$

$$-\sum_{\substack{i=O(k)\\ j\in V_{PN}}} z^1_{ij}\,\overline{f}_k \le f_k \le \sum_{\substack{i=O(k)\\ j\in V_{PN}}} z^1_{ij}\,\overline{f}_k, \quad \forall k\in E_{GN} \tag{82}$$

$$-\sum_{\substack{i=D(k)\\ j\in V_{PN}}} z^1_{ij}\,\overline{f}_k \le f_k \le \sum_{\substack{i=D(k)\\ j\in V_{PN}}} z^1_{ij}\,\overline{f}_k, \quad \forall k\in E_{GN} \tag{83}$$

$$z^1_{ij} \le y^1_{ij}, \quad \forall i\in V_{GN},\,\forall j\in V_{PN} \tag{84}$$

$$z^1_{ij} \le \delta^{PN}_j, \quad \forall i\in V_{GN},\,\forall j\in V_{PN} \tag{85}$$

$$z^1_{ij} \ge y^1_{ij} + \delta^{PN}_j - 1, \quad \forall i\in V_{GN},\,\forall j\in V_{PN} \tag{86}$$

$$z_{ij}^2 \leq y_{ij}^2, \quad \forall i \in V_{PN}, \forall j \in V_{GN} \tag{87}$$

$$z_{ij}^2 \leq \delta_j^{GN}, \quad \forall i \in V_{PN}, \forall j \in V_{GN} \tag{88}$$

$$z_{ij}^2 \geq y_{ij}^2 + \delta_j^{GN} - 1, \quad \forall i \in V_{PN}, \forall j \in V_{GN} \tag{89}$$

$$r_{ijk} \leq z_{jk}^1, \ \ \forall i \in V_{PN}, \forall j \in V_{GN}, \forall k \in V_{PN} \tag{90}$$

$$r_{ijk} \leq y_{ij}^2, \ \ \forall i \in V_{PN}, \forall j \in V_{GN}, \forall k \in V_{PN} \tag{91}$$

$$r_{ijk} \geq z_{jk}^1 + y_{ij}^2 - 1, \forall i \in V_{PN}, \forall j \in V_{GN}, \forall k \in V_{PN} \tag{92}$$

$$z_{ij}^1, z_{ij}^2, r_{ijk} \in \{0, 1\}, \forall i \in V_{PN}, \forall j \in V_{GN}, \forall k \in V_{PN} \tag{93}$$

APPENDIX D
IPGN PARAMETERS

TABLE III: Production capacity and base requested demand for each node in the power network.

Node index	$\overline{\mathbf{p}}_\mathbf{i}$	$\overline{\mathbf{d}}_\mathbf{i}^\mathbf{b}$
1	42	8.5
2	42	8.5
3	42	8.5
4	0	8.5
5	0	8.5
6	42	8.5
7	0	8.5
8	42	8.5
9	0	8.5
10	0	8.5
11	0	8.5
12	0	8.5
13	0	8.5
14	0	8.5

TABLE IV: Boundaries, maximum flow capacity and reactance for each line in the power network.

Line index	Boundaries $(\mathbf{i}, \mathbf{j})$	$\overline{\mathbf{f}}_\mathbf{k}$	$\mathbf{x}_\mathbf{k}$ (p.u.)
1	(1, 2)	30	0.05917
2	(1, 5)	30	0.22304
3	(2, 3)	30	0.19797
4	(2, 4)	30	0.17632
5	(2, 5)	30	0.17388
6	(3, 4)	30	0.17103
7	(4, 5)	30	0.04211
8	(4, 7)	30	0.20912
9	(4, 9)	30	0.55618
10	(5, 6)	30	0.24202
11	(6, 11)	30	0.1989
12	(6, 12)	30	0.25581
13	(6, 13)	30	0.13027
14	(7, 8)	30	0.17615
15	(7, 9)	30	0.11001
16	(9, 10)	30	0.0845
17	(9, 14)	30	0.27038
18	(10, 11)	30	0.19207
19	(12, 13)	30	0.19988
20	(13, 14)	30	0.34802

TABLE V: Production capacity and base requested demand for each node in the gas network.

Node index	$\overline{\mathbf{p}}_\mathbf{i}$	$\overline{\mathbf{d}}_\mathbf{i}$
1	15	0
2	15	0
3	15	0
4	0	5
5	0	5
6	0	5
7	0	5
8	0	5
9	0	5

TABLE VI: Boundaries and maximum flow capacity for each line in the gas network.

Line index	Boundaries $(\mathbf{i}, \mathbf{j})$	$\overline{\mathbf{f}}_\mathbf{k}$
1	(1, 2)	15
2	(1, 5)	10
3	(2, 3)	10
4	(2, 4)	15
5	(2, 5)	10
6	(3, 4)	10
7	(4, 5)	15
8	(4, 7)	10
9	(4, 9)	10

REFERENCES

[1] Z. Guo and Y. Y. Haimes, "Exploring systemic risks in systems-of-systems within a multiobjective decision framework," *IEEE Transactions on Systems, Man, and Cybernetics: Systems*, vol. 47, no. 6, pp. 906–915, 2016.

[2] M. Ouyang, "Review on modeling and simulation of interdependent critical infrastructure systems," *Reliability engineering & System safety*, vol. 121, pp. 43–60, 2014.

[3] S. Corsi and C. Sabelli, "General blackout in italy sunday september 28, 2003, h. 03: 28: 00," in *IEEE Power Engineering Society General Meeting, 2004.* IEEE, 2004, pp. 1691–1702.

[4] S. M. Rinaldi, J. P. Peerenboom, and T. K. Kelly, "Identifying, understanding, and analyzing critical infrastructure interdependencies," *IEEE control systems magazine*, vol. 21, no. 6, pp. 11–25, 2001.

[5] S. V. Buldyrev, R. Parshani, G. Paul, H. E. Stanley, and S. Havlin, "Catastrophic cascade of failures in interdependent networks," *Nature*, vol. 464, no. 7291, pp. 1025–1028, 2010.

[6] E. E. Lee II, J. E. Mitchell, and W. A. Wallace, "Restoration of services in interdependent infrastructure systems: A network flows approach," *IEEE Transactions on Systems, Man, and Cybernetics, Part C (Applications and Reviews)*, vol. 37, no. 6, pp. 1303–1317, 2007.

[7] A. Vespignani, "The fragility of interdependency," *Nature*, vol. 464, no. 7291, pp. 984–985, 2010.

[8] S. V. Buldyrev, N. W. Shere, and G. A. Cwilich, "Interdependent networks with identical degrees of mutually dependent nodes," *Physical Review E*, vol. 83, no. 1, p. 016112, 2011.

[9] R. Parshani, S. V. Buldyrev, and S. Havlin, "Interdependent networks: Reducing the coupling strength leads to a change from a first to second order percolation transition," *Physical review letters*, vol. 105, no. 4, p. 048701, 2010.

[10] M. Ouyang and L. Dueñas-Osorio, "An approach to design interface topologies across interdependent urban infrastructure systems," *Reliability Engineering & System Safety*, vol. 96, no. 11, pp. 1462–1473, 2011.

[11] J. Winkler, L. Dueñas-Osorio, R. Stein, and D. Subramanian, "Interface network models for complex urban infrastructure systems," *Journal of Infrastructure Systems*, vol. 17, no. 4, pp. 138–150, 2011.

[12] G. G. Brown, W. M. Carlyle, J. Salmerón, and K. Wood, "Analyzing the vulnerability of critical infrastructure to attack and planning defenses," in *Emerging Theory, Methods, and Applications*. Informs, 2005, pp. 102–123.

[13] Y.-P. Fang and E. Zio, "An adaptive robust framework for the optimization of the resilience of interdependent infrastructures under natural

hazards," *European Journal of Operational Research*, vol. 276, no. 3, pp. 1119–1136, 2019.
[14] M. Ouyang, "A mathematical framework to optimize resilience of interdependent critical infrastructure systems under spatially localized attacks," *European Journal of Operational Research*, vol. 262, no. 3, pp. 1072–1084, 2017.
[15] J. Beyza, H. F. Ruiz-Paredes, E. Garcia-Paricio, and J. M. Yusta, "Assessing the criticality of interdependent power and gas systems using complex networks and load flow techniques," *Physica A: Statistical Mechanics and its Applications*, vol. 540, p. 123169, 2020.
[16] H. Zhang, P. Wang, S. Yao, X. Liu, and T. Zhao, "Resilience assessment of interdependent energy systems under hurricanes," *IEEE Transactions on Power Systems*, vol. 35, no. 5, pp. 3682–3694, 2020.
[17] J. Johansson, H. Hassel, and A. Cedergren, "Vulnerability analysis of interdependent critical infrastructures: case study of the swedish railway system," *International journal of critical infrastructures*, vol. 7, no. 4, pp. 289–316, 2011.
[18] L. Svegrup and J. Johansson, "Vulnerability analyses of interdependent critical infrastructures: Case study of the swedish national power transmission and railway system," in *European Safety and Reliability Conference (ESREL2015)*. ESREL2015, 2015, pp. 4499–4507.
[19] X. He and E. J. Cha, "Modeling the damage and recovery of interdependent critical infrastructure systems from natural hazards," *Reliability Engineering & System Safety*, vol. 177, pp. 162–175, 2018.
[20] H. Guo, S. S. Yu, H. H. Iu, T. Fernando, and C. Zheng, "A complex network theory analytical approach to power system cascading failure—from a cyber-physical perspective," *Chaos: An Interdisciplinary Journal of Nonlinear Science*, vol. 29, no. 5, p. 053111, 2019.
[21] S. Wang, L. Hong, and X. Chen, "Vulnerability analysis of interdependent infrastructure systems: A methodological framework," *Physica A: Statistical Mechanics and its applications*, vol. 391, no. 11, pp. 3323–3335, 2012.
[22] Z. Chen, J. Wu, Y. Xia, and X. Zhang, "Robustness of interdependent power grids and communication networks: A complex network perspective," *IEEE Transactions on Circuits and Systems II: Express Briefs*, vol. 65, no. 1, pp. 115–119, 2017.
[23] D. F. Rueda and E. Calle, "Using interdependency matrices to mitigate targeted attacks on interdependent networks: A case study involving a power grid and backbone telecommunications networks," *International Journal of Critical Infrastructure Protection*, vol. 16, pp. 3–12, 2017.
[24] S. G. Nurre, B. Cavdaroglu, J. E. Mitchell, T. C. Sharkey, and W. A. Wallace, "Restoring infrastructure systems: An integrated network design and scheduling (inds) problem," *European journal of operational research*, vol. 223, no. 3, pp. 794–806, 2012.
[25] M. Ouyang and Y. Fang, "A mathematical framework to optimize critical infrastructure resilience against intentional attacks," *Computer-Aided Civil and Infrastructure Engineering*, vol. 32, no. 11, pp. 909–929, 2017.
[26] A. D. González, L. Dueñas-Osorio, M. Sánchez-Silva, and A. L. Medaglia, "The interdependent network design problem for optimal infrastructure system restoration," *Computer-Aided Civil and Infrastructure Engineering*, vol. 31, no. 5, pp. 334–350, 2016.
[27] Y.-P. Fang, G. Sansavini, and E. Zio, "An optimization-based framework for the identification of vulnerabilities in electric power grids exposed to natural hazards," *Risk Analysis*, vol. 39, no. 9, pp. 1949–1969, 2019.
[28] Y. Fang and G. Sansavini, "Optimizing power system investments and resilience against attacks," *Reliability Engineering & System Safety*, vol. 159, pp. 161–173, 2017.
[29] L. Zhao and B. Zeng, "Vulnerability analysis of power grids with line switching," *IEEE Transactions on Power Systems*, vol. 28, no. 3, pp. 2727–2736, 2013.
[30] ——, "An exact algorithm for two-stage robust optimization with mixed integer recourse problems," *submitted, available on Optimization-Online. org*, 2012.
[31] B. Zeng and L. Zhao, "Solving two-stage robust optimization problems using a column-and-constraint generation method," *Operations Research Letters*, vol. 41, no. 5, pp. 457–461, 2013.
[32] M. E. Newman, "Mixing patterns in networks," *Physical review E*, vol. 67, no. 2, p. 026126, 2003.
[33] L. Gurobi Optimization, "Gurobi optimizer reference manual," 2021. [Online]. Available: http://www.gurobi.com